Agroforestry Systems **63:** 133–147, 2004.

Three-dimensional aerodynamic structure of a tree shelterbelt: Definition, characterization and working models

X.H. Zhou[1,*], J.R. Brandle[1], C.W. Mize[2] and E.S. Takle[3]

[1]School of Natural Resources, University of Nebraska, 03 Plant Industry, East Campus, Lincoln, NE 68583-0814, USA; [2]Department of Natural Resource Ecology and Management, Iowa State University, Ames, IA 50011, USA; [3]Department of Geological and Atmospheric Sciences and Department of Agronomy, Iowa State University, Ames, IA 50011, USA; [*]Author for correspondence (tel.: +1-402-472-9889; fax: +1-402-472-2964; e-mail: xzhou2@unl.edu)

Received 10 May 2001; accepted in revised form 12 January 2004

Key words: Cubic density, Cubic porosity, Optical density, Optical porosity, Vegetative surface area density, Windbreak(s)

Abstract

In order to make recommendations to landowners with regard to the design and management of tree shelterbelts, it is necessary to understand and predict the wind flow patterns associated with shelterbelt structure. A structural description is a prerequisite for any prediction of wind flow. Optical porosity (percentage of open spaces on the side view of a shelterbelt) has been used as a structural descriptor of a shelterbelt; however, it is a 2-dimensional measure unable to fully represent the aerodynamic influence of a tree shelterbelt. Based on numerous studies observing the wind fields associated with shelterbelt structure, the overall aerodynamic structure of a tree shelterbelt in three dimensions is defined by its external structural characteristics (length, height, width, and cross-sectional shape) and by its internal structural components (amounts and arrangements of vegetative surface area and volume, and geometric shape of individual vegetative elements). In order to associate the defined structure with wind speed, turbulent stress, and pressure, it is characterized using two structural descriptors: the spatial functions of vegetative surface area density (vegetative surface area per unit canopy volume) and cubic density (vegetative volume per unit canopy volume). For field estimation, the two structural descriptors are expressed in three dimensions using two working models in terms of 1- or 2- dimensional sub-functions capable of being defined with field measurements. This paper discusses the rationale behind the definition, characterization, and working models for the 3-dimensional aerodynamic structure of a tree shelterbelt.

Introduction

Shelterbelts or windbreaks are barriers used to reduce wind speed and alter wind fields. As a result of the changes in wind flow patterns, microclimate in the protected zone is altered. The wind flow modification of a particular shelterbelt is dependent on its structure (Heisler and DeWalle 1998). Different structural designs provide different wind flow patterns, allowing different landowner objectives to be met (Woodruff et al. 1963).

Most of these design considerations are met by manipulating species selection, shelterbelt location, and planting pattern (Cao et al. 1981a). When these factors are changed, the amount and arrangement of the vegetative elements within the shelterbelt are changed. This, in turn, alters the path of the wind flow through or around the barrier, resulting in variations in the quantity and quality of protection provided by the shelterbelt. Knowing how to manipulate shelterbelt structure to meet specific objectives is one criti-

cal requirement for helping landowners manage shelterbelts (Brandle et al. 2000).

Shelterbelt structure is defined as the amount and arrangement of plant elements and the open spaces between these elements (Sturrock 1969; Zhang et al. 1995). Optical porosity (the percentage of open space as seen perpendicularly to the shelterbelt side) and optical density (the percentage of the solid portion) of a shelterbelt are commonly used structural descriptors for a shelterbelt (Loeffler et al. 1992). When a barrier is a slat fence with no significant width dimension, optical porosity provides an excellent measure of structure and a reasonable approximation of the path of wind flow through the fence. In this case, optical porosity has been used successfully to predict the wind fields around a 2-dimensional (2D) fence by its parameterization of the drag force in the equations of motion (Wilson 1987).

In the case of a tree shelterbelt, two shelterbelts with similar optical porosities may have very different external characteristics and different internal vegetative surface areas and volumes. Furthermore, the arrangement of plant elements or open spaces within their canopies is likely to be different, which suggests that they have different aerodynamic properties and hence different flow patterns in the sheltered area. As a better understanding of the turbulent flows through a shelterbelt developed, limitations of optical porosity as a structural descriptor for a tree shelterbelt became apparent (Zhang et al. 1995). Moreover, the simulation of 3-dimensional (3D) boundary-layer flows around a shelterbelt is a topic where continued research is required (Judd et al. 1996). Therefore, being able to define the aerodynamic structure of a tree shelterbelt in three dimensions provides a better basis for predicting wind flow associated with the overall structure of a tree shelterbelt.

In this paper, we re-analyze data from papers relating shelterbelt structure to aerodynamic responses and define the 3D aerodynamic structure of a tree shelterbelt. Further, in order to be useful to research and management communities, the structural descriptors characterizing the defined structure must be developed and expressed in easily used models.

Data acquisition

The data presented in this paper were either directly taken from previously published papers or indirectly scaled from the figures in those papers using a digital caliper with an accuracy of 0.01 mm. Optical porosities of shelterbelts were given in most of the original papers. In other cases (Woodruff and Zingg 1952; Jensen 1954; Woodruff et al. 1963; Surrock 1969, 1972), optical porosities were estimated from their published photos using the cluster method in MultiSpec© image analysis software (Loeffler et al. 1992). Parameters in the models used to describe the relationship between optical porosity of a shelterbelt and its aerodynamic response were estimated using the Marquardt method in the NLIN Procedure of SAS©.

Motivation for improving shelterbelt structural description

Comparison of the data in Figures 1 to 3 illustrates that shelterbelts with similar optical porosities have very different aerodynamic influences as indicated by conventional measures of shelter effectiveness. The aerodynamic terms of these measures are minimum relative wind speed (the ratio of leeward minimum wind speed to open wind speed at the same height (Figure 1)), average reduction of relative wind speed (the ratio of leeward wind speed to open wind speed at the same height) over 25 H (where H is barrier height) in the lee (Figure 2), and 70% effectively protected distance (the leeward horizontal distance within which the relative wind speed is less than 70% (Figure 3)). Regression analyses did a fair job of assessing average trends of these three aerodynamic terms versus optical porosity. However, the percentages of variance explained by regression in all three cases were less than 52% due to the significant variability of each aerodynamic term at a given optical porosity.

The data in Figures 1 to 3 were collected from 19 publications. In these publications, the instrumentation, measurement height, local surface condition, and turbulence regime of the approaching flow were different. If not caused by these four factors, significant variability of an aerodynamic term at a given optical porosity in Figures 1 to 3 was caused by the inability of optical porosity to sufficiently specify the shelter effect of a barrier with significant width. We assumed the instrumentation used by different studies met the standard of accuracy of the time and should not cause significant variability of measured wind flow. The measurement height was not a factor contributing to variability of the data in Figures 1 to 3, because the three figures were all derived from the relative wind

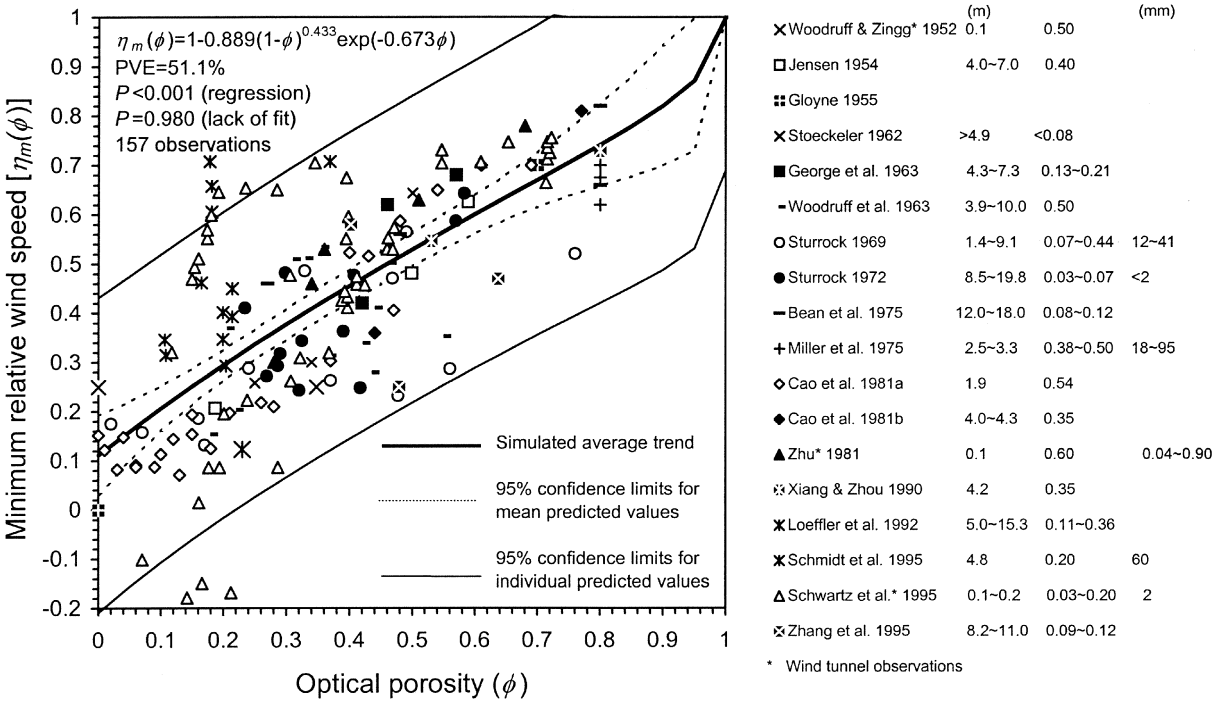

	H (m)	z/H	z_0 (mm)
×Woodruff & Zingg* 1952	0.1	0.50	
□Jensen 1954	4.0~7.0	0.40	
⁘Gloyne 1955			
×Stoeckeler 1962	>4.9	<0.08	
■George et al. 1963	4.3~7.3	0.13~0.21	
-Woodruff et al. 1963	3.9~10.0	0.50	
○Sturrock 1969	1.4~9.1	0.07~0.44	12~41
●Sturrock 1972	8.5~19.8	0.03~0.07	<2
–Bean et al. 1975	12.0~18.0	0.08~0.12	
+Miller et al. 1975	2.5~3.3	0.38~0.50	18~95
◇Cao et al. 1981a	1.9	0.54	
◆Cao et al. 1981b	4.0~4.3	0.35	
▲Zhu* 1981	0.1	0.60	0.04~0.90
⊠Xiang & Zhou 1990	4.2	0.35	
✱Loeffler et al. 1992	5.0~15.3	0.11~0.36	
✱Schmidt et al. 1995	4.8	0.20	60
△Schwartz et al.* 1995	0.1~0.2	0.03~0.20	2
⊠Zhang et al. 1995	8.2~11.0	0.09~0.12	

* Wind tunnel observations

Figure 1. The relationship of optical porosity to minimum relative wind speed leeward of the barrier with a significant width dimension (H is barrier height; z, measurement height; z_0, the roughness length; and PVE, the percentage of variance explained by regression).

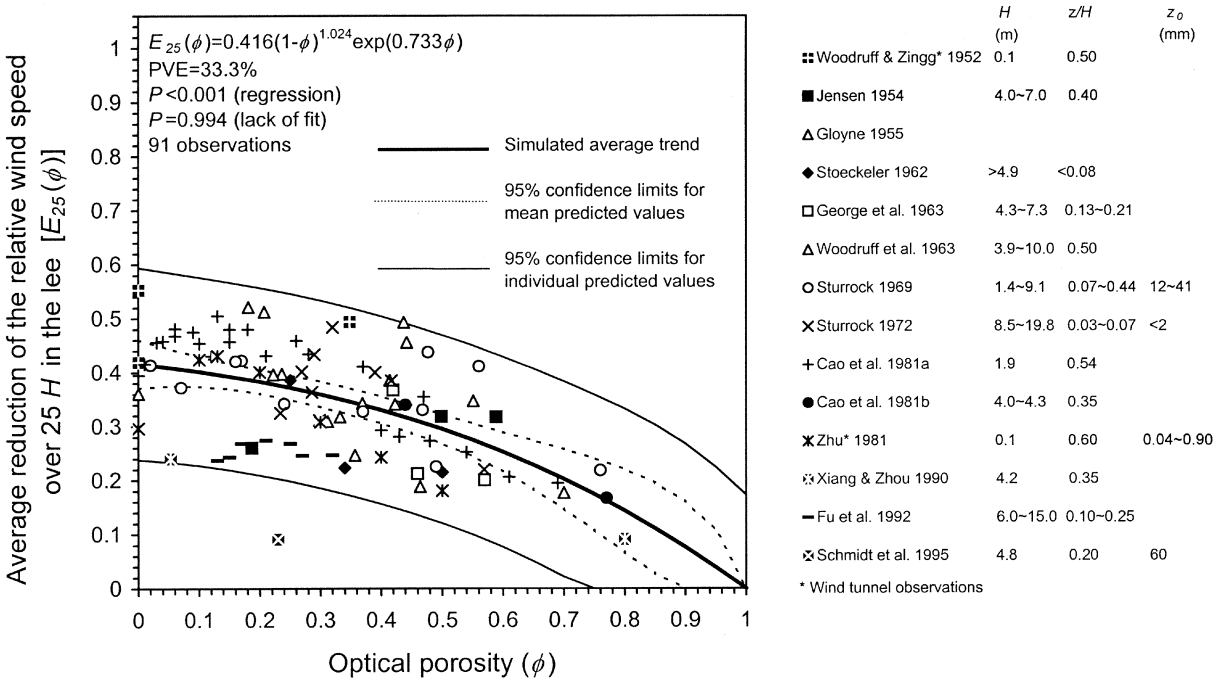

	H (m)	z/H	z_0 (mm)
⁘Woodruff & Zingg* 1952	0.1	0.50	
■Jensen 1954	4.0~7.0	0.40	
△Gloyne 1955			
◆Stoeckeler 1962	>4.9	<0.08	
□George et al. 1963	4.3~7.3	0.13~0.21	
△Woodruff et al. 1963	3.9~10.0	0.50	
○Sturrock 1969	1.4~9.1	0.07~0.44	12~41
×Sturrock 1972	8.5~19.8	0.03~0.07	<2
+Cao et al. 1981a	1.9	0.54	
●Cao et al. 1981b	4.0~4.3	0.35	
✱Zhu* 1981	0.1	0.60	0.04~0.90
⊠Xiang & Zhou 1990	4.2	0.35	
–Fu et al. 1992	6.0~15.0	0.10~0.25	
⊠Schmidt et al. 1995	4.8	0.20	60

* Wind tunnel observations

Figure 2. The relationship of optical porosity to average reduction of relative wind speed over 25 H in the lee of the barrier with a significant width dimension (H is barrier height; z, measurement height; z_0, the roughness length; and PVE, the percentage of variance explained by regression).

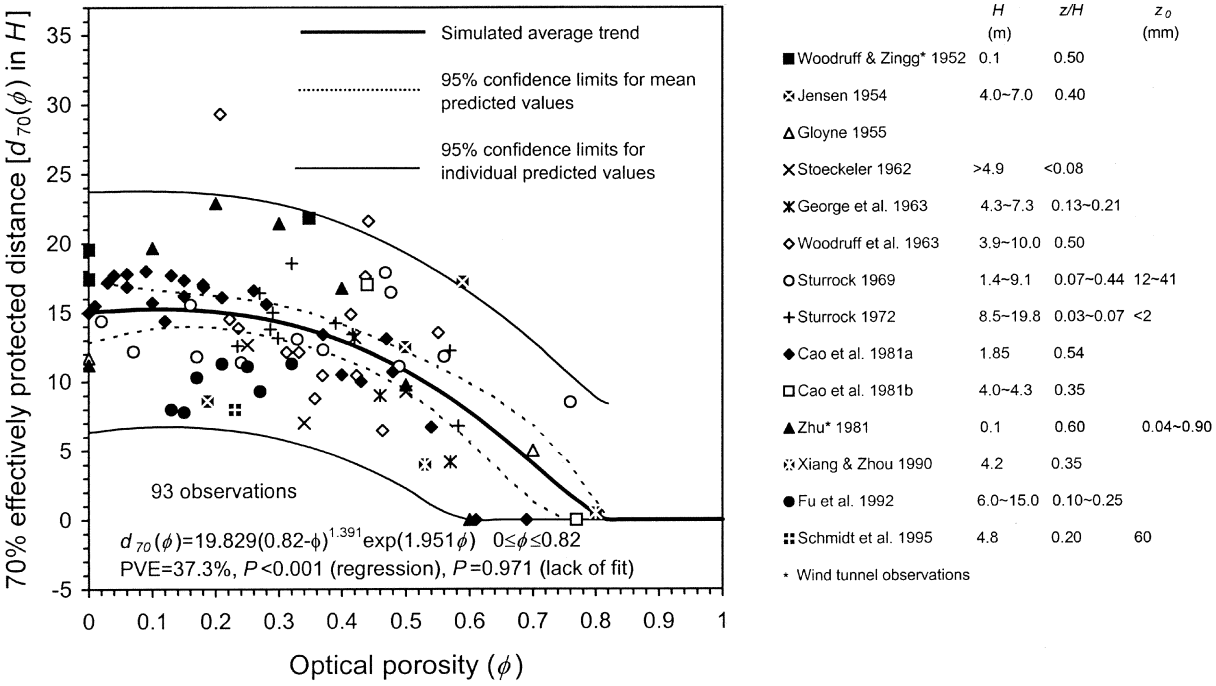

Figure 3. The relationship of optical porosity to 70% effectively protected distance leeward of the barrier with a significant width dimension (H is barrier height; z, measurement height; z_0, the roughness length; and PVE, the percentage of variance explained by regression).

speed measured at low levels where the relative wind speed is independent of height. The data points of relative wind speed measured at the different heights (below 0.6 H in a smooth wind tunnel (Figure 170 in Jensen (1954)), below 0.4 H in a rough wind tunnel (Figure 171 in Jensen (1954)), or below 0.56 H in the field (Figure 4 in Heisler and DeWalle 1988)) all fell on the same curve when plotted against horizontal distance from a shelterbelt (see also Figure 5 in Bean et al. 1975). The importance of the local surface condition and the turbulence regime were recognized in the modelling process (Judd et al. 1996); however, few field studies provided these descriptions. Therefore, the data in Figures 1 to 3 could not be scaled and normalized to account for variations in the terrain roughness or the turbulence regime, which may add to variability in the figures. However, this variability should not be significant because most terrains chosen for measurements of wind speed were flat with minimum roughness, and most of these measurements were made under neutral atmospheric stability. Minimizing the potential influence of the four factors to cause significant variability of an aerodynamic term at given optical porosity in Figures 1 to 3, we conclude that optical porosity as a 2D structural descriptor is unable to sufficiently represent the aerodynamic structure of a tree shelterbelt.

This limitation was recognized by earlier researchers and led to the introduction of various alternative descriptors, including *body of gaps* (Sturrock 1969), *standing woody density* (Cao et al. 1981a), *aerodynamic porosity* (Loeffler et al. 1992), and *3D porosity* (Zhang et al. 1995). Unfortunately, these structural descriptors were not widely accepted, perhaps because their aerodynamic implications were not well addressed relative to the structural components of the shelterbelt. Nevertheless, their introduction indicates the need to define the aerodynamic structure of a tree shelterbelt in three dimensions and to find more accurate structural descriptors as substitutes for optical porosity. These structural descriptors should be defined on a basis of underlying aerodynamic influences of the structural components and should be accurately related to the aerodynamic influence of a tree shelterbelt.

Aerodynamic influence of the overall shelterbelt structure

The overall structure of a tree shelterbelt in three dimensions is represented by its external structural characteristics including length, height, width, cross-sectional shape, and orientation and by its internal structural components including vegetative surface area and volume as well as the arrangement and geometrical shapes of the vegetative elements.

Aerodynamic influence of the external structural characteristics of a shelterbelt

Aerodynamic influence of shelterbelt length and height

The length of a tree shelterbelt is set by its design. The height, however, is dependent on tree species, age, planting pattern, and site condition. Both length and height determine the extent of the sheltered areas. The fields of wind speed as influenced by a shelterbelt are all described in one dimension (with height or across width) or in two dimensions (height-width domain). Ignoring the effects of the two shelterbelt ends on a wind flow field, the descriptions assume that the shelterbelt length is long enough and the proportion of the sheltered area influenced by the two shelterbelt ends is small and negligible so that the influence along length is uniform. However, this assumption is not valid in the case of short barriers commonly existing around farmsteads. To address the variability in the wind field along length or in three dimensions for any shelterbelt, the length of the shelterbelt needs to be specified.

Shelterbelt height is used universally as a scale factor for wind fields, sometimes with the specification of H/z_0 where z_0 is the roughness length of H/L where L is the Monin-Obukhov length. This means that the height of any shelterbelt is unity in the scaled space, and that its scaled aerodynamic influence is independent of height with a given atmospheric stability (H/L) of the approaching flow and surface roughness (H/z_0). This conditional independence of shelterbelt aerodynamics on height is conventionally accepted but has not been theoretically proven.

Tabler and Veal (1971) measured the vertical profiles of wind speed at three leeward locations: 2.5 H, 5 H, and 10 H from each of five fences with different heights. They found that the relative wind speed reduction factor $(1-\int_0^H u(z)dz/\int_0^H u_0(z)dz$, where $u(z)$ and $u_0(z)$ are wind speeds at height of z in the sheltered and unsheltered areas, respectively) in the identical locations behind the five fences was not constant. However, it was a function of fence height. In addition, the ratio of wind speed reduction factor to fence height decreased with increasing fence height (Figure 2 and Figure 4 in Tabler and Veal (1971)). This observed evidence does not support the conditional independence of shelterbelt aerodynamics on height and suggests that shelterbelt height should be included in defining the 3D aerodynamic structure.

Aerodynamic influence of shelterbelt orientation

The aerodynamic influence of a shelterbelt varies with the incident angle of the approaching wind (Schmidt et al. 1995). The aerodynamic influences of shelterbelt orientation are addressed relative to the direction of the approaching wind. Thus, shelterbelt orientation alone does not have any aerodynamic implication, which allows us to ignore the shelterbelt orientation in defining the 3D aerodynamic structure.

Aerodynamic influence of shelterbelt width

The width of a tree shelterbelt is a function of its age, species composition, number of rows, planting patterns, and management. Takahashi (1978) and Wang et al. (2001) studied the aerodynamic influence of the shelterbelts with different widths. Keeping the element surface area and volume constant across the width dimension, both studies arrived at nearly the same conclusion that the aerodynamic influence of width was insignificant. The tree shelterbelts with different widths (different numbers of rows), but the same age, species composition, spacing, planting pattern, and management should have similar amounts of vegetative surface area and volume in a unit canopy volume, depending on genetic uniformity of species, thus total vegetative surface area and volume within their canopies are not constant, but increase with their widths. Apparently, the conclusions from the two studies apply primarily to the theoretical situation rather than to a tree shelterbelt. Other studies have shown that the turbulence fields influenced by barriers with significant width were quite different from those influenced by barriers without significant width (Woodruff and Zingg 1952, 1953; Schwartz et al. 1995). Therefore, width of a tree shelterbelt must have significant aerodynamic influence.

A: Calculated using data from Woodruff and Zingg (1953)

Shapes	$\eta_m(0.5)$	$d_{75}(0.5)$ H	$E_{25}(0.5)$	$R_{10}(0.5)$ H^{-1}
a	0.25	21.44	0.48	0.035
b	0.23	24.80	0.55	0.028
c	0.19	27.64	0.57	0.017
d	0.12	24.05	0.56	0.045

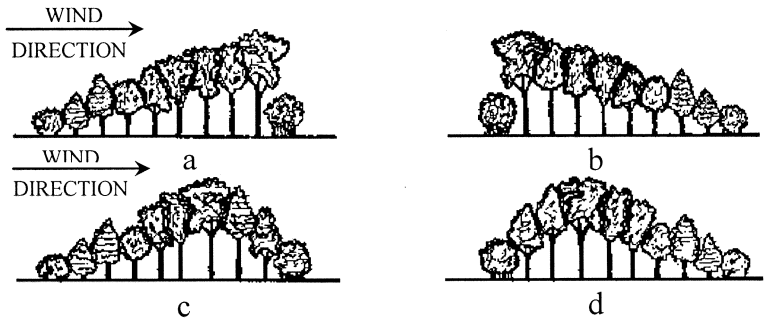

B: Calculated using data from Cao et al. (1981a)

Shapes	$\eta_m(0.54)$	$d_{70}(0.54)$ H	$E_{25}(0.54)$	$R_{10}(0.54)$ H^{-1}
a	0.63	3.31	0.19	0.022
b	0.48	5.41	0.21	0.037
c	0.49	6.89	0.22	0.035
d	0.16	6.80	0.43	0.046
e	0.57	4.48	0.18	0.026

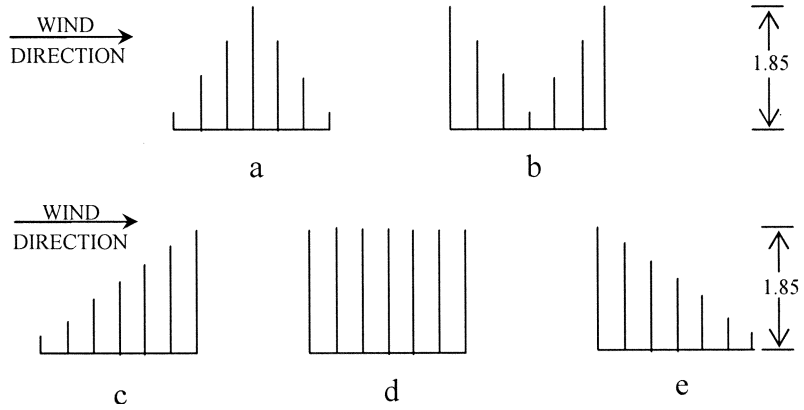

Figure 4. The shelter effectiveness of the model shelterbelts with different cross-sectional shapes [$\eta_m(z)$ is minimum relative wind speed in the lee where z is measurement height in barrier height (H); $d_{70}(z)$ or $d_{75}(z)$, 70% or 75% effectively protected distance; $E_{25}(z)$, average reduction of relative wind speed over 25 H in the lee; and $R_{10}(z)$, recovery rate of the wind speed 10 H downwind of its minimum towards equilibrium].

Aerodynamic influence of the cross-sectional shape of a shelterbelt

The cross-sectional shape of a tree shelterbelt is the external profile of its cross-section and is determined by its width, height, and the geometry of its boundary. Various shapes of tree shelterbelts are formed by the planting patterns of trees and/or shrubs, by species composition, or by removal or addition of trees and/or shrubs. The aerodynamic influence of the cross-sectional shape of a shelterbelt was recognized by earlier shelterbelt ecologists. The shelterbelt with a streamlining shape in its cross-section, which appears as a pitched or gable roof with a wide sweep in the eaves, has been frequently advocated. This is often achieved by planting central rows with tall trees and by flanking shorter trees and/or shrubs on either side (Caborn 1960).

Woodruff and Zingg (1953) and Cao et al. (1981a) investigated the aerodynamic influence of shelterbelts with different cross-sectional shapes, but with equal heights, lengths, and widths. Using their data, we calculated shelter effectiveness shown in Figure 4A and Figure 4B. These results show that shelterbelts with different cross-sectional shapes have very different aerodynamic influences on minimum relative wind speed, 70% or 75% effectively protected distance, average reduction of the relative wind speed over 25 H in the lee, and recovery rate of wind speed 10 H downwind of its minimum towards equilibrium (the ratio of an increment in the relative wind speed over 10 H downwind of its minimum to 10 H).

Aerodynamic influence of the internal structural components of a shelterbelt

Aerodynamic influence of the vegetative surface area within a shelterbelt canopy

Vegetative surfaces extract momentum from and exert a shear stress on the wind flow. Wilson and Shaw (1977) asserted that the mean spatial derivative of pressure fluctuations in a canopy was not zero as traditionally accepted, but that it was the pressure force that constituted the major portion of the total drag force of vegetation. They proposed that this drag force was dependent on the vegetative surface area density (S_{AD}), defined as vegetative surface area per unit canopy volume, and the velocity of air flow (u_i) such that:

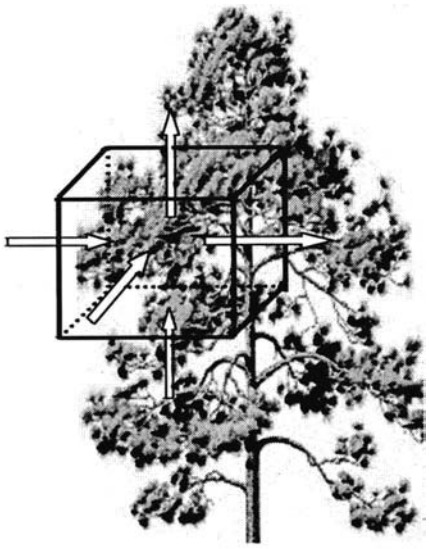

Figure 5. Diagram of air flow into and out of a cube filled with vegetative elements (arrows indicate the direction of air motion).

$$\overline{\frac{\partial \rho'}{\partial x_i}} = C_D S_{AD} \bar{u}_i^2 \tag{1}$$

where overbar ($\bar{}$) denotes the spatial average; prime ($'$), the departure of a variable from its average; p, pressure; x_i (i = 1, 2 and 3), the coordinate in the ith dimension; and C_D, the surface drag coefficient. Thereafter, vegetative surface area density was widely accepted as a major aerodynamic structural descriptor not only for homogenous canopies, but also for linear shelterbelt canopies. It was used to parameterize the drag force in the equations of motion for simulating the turbulent flow around a shelterbelt (Wang et al. 2001), in and over a homogenous canopy (Lee 2000), and around a single tree (Gross 1987).

Aerodynamic influence of the vegetative volume within a shelterbelt canopy

Divergence and convergence of air flow inside a shelterbelt canopy are results of flow around solid portions and through void spaces. Consider a given cube within a tree canopy (Figure 5). If air enters the cube with the same velocity in three directions, more air enters the cube from the side where vegetative volume is least. Similarly, if air leaves the cube with the same velocity in the three directions, less air flow leaves the cube from the side where vegetative volume is greatest.

The pressure decrease of fluid flow through a porous medium is determined not only by the surface area of the medium but also by the solid volume of the medium. Kozeny (1927) expressed this pressure decrease in terms of cubic porosity and surface area density, assuming that the porous medium was represented by an assemblage of crooked channels of various cross-sections and lengths. Cubic porosity is a measure of the void spaces among the solid portions in a unit medium volume, that function as the passages through which fluid flows. Surface area density is a measure of the surface areas in contact with the fluid flow in a unit medium volume, that extract momentum from and exert shear stress on the fluid flow. Therefore, in Kozeny's formula, the pressure decrease of the fluid flow through a porous medium is directly proportional to its surface area density and inversely proportional to its cubic porosity (Scheidegger 1974).

While cubic porosity has not yet been reported as a structural descriptor for shelterbelts, it was used as a structural descriptor for a tree crown to simulate the wind fields around individual trees with different crown shapes (Gross 1987).

Aerodynamic influence of the arrangement of shelterbelt elements

The arrangement of the vegetative elements within a tree shelterbelt can be described by the spatial distributions of vegetative surface area and volume. The distribution of vegetative surface area in a shelterbelt canopy spatially represents the momentum sinks and shear stress sources for the wind flow. In locations where vegetative surface area per unit volume is high, wind flow loses more momentum due to surface drag. The distribution of vegetative volume in a shelterbelt canopy is responsible for the divergence and convergence of air flow. At a given velocity, more air converges through the more permeable portions where there is less vegetative volume and diverges around the denser portions where vegetative volume is greater.

The wind speed reduction and the size of the protected zone, as influenced by a fence with a uniform porosity, are different from those created by a fence with a non-uniform porosity (Gandemer 1979). As the lower portion of a fence becomes more porous, more air flows through the fence near the ground, increasing the relative wind speed while extending the protected zone further to the lee. As the upper portion of a fence becomes more porous, the pressure gradient between the top of the fence and the ground becomes larger, causing a *Coanda effect*, or a downward flow, increasing turbulence, and shortening the extent of the protected zone (Plate 1971).

Wilson (1987) compared the boundary-layer flows as influenced by fences having uniform and non-uniform optical porosities. Both fences had an overall optical porosity of 0.5, but the non-uniform one had increasing optical porosity with height. Within 6 H leeward, the uniform fence had greater wind speed reduction at a height of 1 H but less at 0.5 H than the non-uniform one. The energy spectra of vertical velocity behind the two fences were clearly distinguishable (Figure 7b in Wilson (1987)).

Aerodynamic influence of the geometric shape of shelterbelt elements

The geometric shape of an element is a factor determining its drag force on fluid flow. Elements with rounded edges, such as branches, tend to have less drag than those with sharp edges, such as slates in a board fence (Heisler and DeWalle 1988). Similarly, the geometric shape of the openings between elements has an influence on the flow through those openings. It appears, however, that the effect is limited to the area near a barrier. As distance from the barrier increases, the influence of geometric shape of elements inside the barrier on flow pattern attenuates (Figure 2 in Perera 1981).

Proposed definition of the 3D aerodynamic structure of a tree shelterbelt

The previous discussion indicates that wind fields around a shelterbelt are comprehensively influenced by its external structural characteristics and internal structural components. In order to more accurately predict the wind fields around a tree shelterbelt, *its overall aerodynamic structure in three dimensions should be defined by its external structural characteristics: length, height, width, and cross-sectional shape; and by its internal structural components: amounts and arrangements of its vegetative surface area and volume as well as the geometric shape of individual elements.* The prediction of wind fields requires the quantitative association of this defined structure with wind speed, turbulent stress, and pressure. Subsequently, the quantitative characterization of the 3D aerodynamic structure becomes essential.

Characterization of the 3D aerodynamic structure of a tree shelterbelt

A tree shelterbelt canopy is often qualitatively described as a porous medium which is defined as a solid body containing pores. Intuitively, the meaning of a pore is quite clear. However, it is difficult to give an exact geometric definition of what is meant by the notion of a pore. Pores are void spaces of various sizes and are distributed more or less irregularly throughout a medium (Scheidegger 1974). Similarly, the pores in a shelterbelt canopy are irregularly distributed and have various sizes with different geometric shapes. Therefore, a tree shelterbelt canopy can be considered as a porous medium.

Within the canopy, vegetative elements are interspersed with pores. These solid elements and pores are arranged in a mixed geometric matrix where the solid/pore interfaces form a complicated surface. Neither the solid/pore interfaces extracting momentum from wind flow, nor the volume arrangement determining the divergence and convergence of wind flow can be described by an analytical equation with infinitely high resolution. However, the total volume of a tree shelterbelt can be considered as a collection of numerous small grid cells. Within each cell, the amounts of vegetative surface area and volume can be defined using area and volume quantities. As the size of each cell becomes infinitely small, the number of grid cells becomes infinitely large, and the surface area and volume determinations, while mathematically possible, become meaningless. For example, the amounts of surface area and volume in an infinitely small cell approach zero, but relative to the size of the cell, both surface area and volume approach either one or zero depending on whether or not the cell is occupied by a solid element. At the other extreme, as the size of each cell becomes large, the ability to describe the arrangements of vegetative surface area and volume within a shelterbelt canopy decreases.

Accordingly, the amounts of vegetative surface area and volume must be defined at a finite resolution as determined by the cell size so as to provide a meaningful measure. The measure of the amounts of vegetative surface area and volume is independent of the resolution if both are defined relative to the cell size. In a cell, vegetative surface area relative to the cell size is vegetative surface area density and vegetative volume relative to the cell size is cubic density (vegetative volume per unit canopy volume). Therefore, vegetative surface area density and cubic density (or cubic porosity) are the two structural descriptors of choice for characterizing the amounts of vegetative surface area and volume.

It is assumed that vegetative elements are randomly and motionlessly distributed within a grid cell. The random assumption suggests that either vegetative surface area density or cubic density in one grid cell can be represented by one value. The motionless assumption means that vegetative surface area, volume, and element composition in a grid cell do not change with respect to time. This is consistent with the flow model assumptions that ignore momentum transfer to plant motion, allowing either vegetative surface area density or cubic density to be expressed as a spatial function independent of time. As spatial functions, vegetative surface area density and cubic density have an obvious advantage and are capable of describing the spatial distributions of vegetative surface area and volume at a given resolution.

Branches and trunks have cylindrical shapes. Leaves are broad and flat, needle-like, or scale-like. Seeds and their assemblage have more complicated shapes, but their amount is small, even negligible (Zhou et al. 2002). It is impractical for the structural characterization to take each geometric shape of individual vegetative elements into account. Elements with different shapes have different surface-to-volume ratios. Accordingly, the vegetative surface area density and cubic density should be able to jointly reflect the geometric shape of vegetative elements. Additionally, both should be able to describe the average size of vegetative elements in a shelterbelt canopy. For example, the elements having greater volume and smaller surface area have a bigger average size than those having smaller volume and greater surface area. Therefore, the spatial variability in a ratio of vegetative surface area density to cubic density should reflect the heterogeneity of the geometric shapes and average sizes of tree components in a shelterbelt canopy.

Defined in the 3D domain containing a shelterbelt canopy, both spatial functions of vegetative surface area density and cubic density are continuously zero outside the boundary of the canopy envelope. Therefore, the influence of the length, height, width, and cross-sectional shape of a shelterbelt can be represented by the surface area density and cubic density at each gird cell in the computational domain. In other words, either term can be used to indicate shelterbelt length, height, width, and cross-sectional shape, as defined by its domain boundary, outside of which the

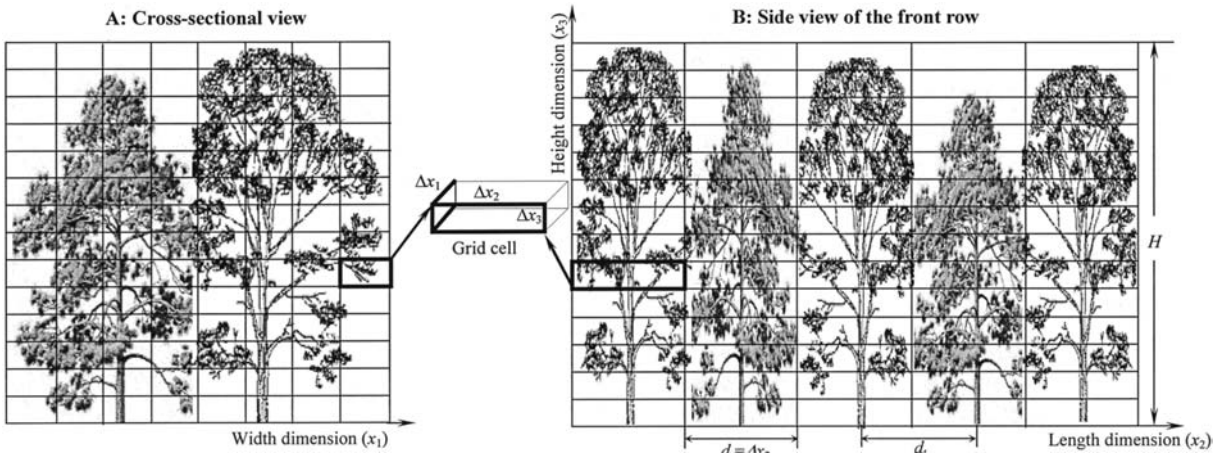

Figure 6. A green ash (*Fraxinus pennsylvanica* Marsh.) and Austrian pine (*Pinus nigra* Arnod) shelterbelt as a collection of the discrete grid cells.

term is continuously zero. For example, if the vegetative surface area density of a shelterbelt canopy is expressed as a spatial function $S_{AD}(D, h, x_1, x_2, x_3)$, then:

$$S_{AD}(D,h,x_1,x_2,x_3) = \begin{cases} f(D,h,x_1,x_2,x_3) \geq 0 & 0 \leq x_1 \leq 10 \text{ or } 0 \leq x_2 \leq 100 \text{ or} \\ & [(x_1-5)^2+(x_3-7)^2 \leq 25 \\ & \text{where } x_3 > 7] \\ 0 & \text{else} \end{cases} \quad (2)$$

where D is DBH (diameter at breast height); h, tree height; and $f(D, h, x_1, x_2, x_3)$, a universal function. Additionally, x_1, x_2 and x_3, are the coordinates in the width, length, and height dimensions. The domain of this function indicates that the length of the shelterbelt is 100; height, 12; width, 10; and cross-sectional shape, an assemblage of a rectangle and the half circle that is on the top of the rectangle. The advantage of the spatial function of vegetative surface area density provided Wang et al. (2001) with the capability of simulating the influence of cross-sectional shape of hypothetical shelterbelts on shelter efficiency.

In summary, the spatial functions of vegetative surface area density and cubic density are the two structural descriptors of choice for characterizing the 3D aerodynamic structure of a tree shelterbelt because they have ability to describe the amounts and arrangements of vegetative surface area and volume in a tree shelterbelt canopy; to jointly reflect the geometric shapes of tree components; and to indicate the length, height, width, and cross-sectional shape of a tree shelterbelt. If both structural descriptors are incorporated into the equations of motion and the continuity equation, the aerodynamic influence of the overall shelterbelt structure on wind speed, turbulent stress, and pressure can be numerically predicted. Our efforts to incorporate these structural descriptors into the equations of motion and continuity equation are reported in Zhou et al. (2004). Any solution to these equations will require estimates for both structural descriptors.

Working models for guiding the field estimation of the structural descriptors

A numerical method to solve the equations of motion along with the continuity equation for simulating the wind fields near a shelterbelt subdivides the shelterbelt and the surrounding space into numerous discrete grid cells (Takle et al. 2003). Accordingly, vegetative surface area density and cubic density in the grid cells in Figure 6 are needed for simulation of the wind fields as influenced by the overall shelterbelt structure. To know both structural descriptors in each grid cell within a tree shelterbelt canopy requires that the vegetative surface area and volume for each tree be expressed in terms of spatial variables (x_1, x_2, x_3). To estimate both structural descriptors for a field shelterbelt also requires that the vegetative surface area and volume for an individual tree be related to easily measured parameters such as DBH and height.

Assuming that an implicit function $S(D, h, x_1, x_2, x_3)$ represents the vegetative surface area in a spatial location (x_1, x_2, x_3) within a crown of a given tree with known DBH and height at a particular site, the vegetative surface area density $S_{AD}(D, h, x_1, x_2, x_3)$ for this tree in a grid cell centered at (x_1, x_2, x_3) with dimensions Δx_1, Δx_2, and Δx_3 (Figure 6) can be expressed as:

$$S_{AD}(D,h,x_1,x_2,x_3) = \frac{1}{\Delta x_1 \Delta x_2 \Delta x_3} \int_{x_3-0.5\Delta x_3}^{x_3+0.5\Delta x_3} \int_{x_2-0.5\Delta x_2}^{x_2+0.5\Delta x_2} \int_{x_1-0.5\Delta x_1}^{x_1+0.5\Delta x_1} S(D,h,x'_1,x'_2,x'_3)dx'_1dx'_2dx'_3 \quad (3)$$

It is difficult to explicitly define the function of vegetative surface area due to the complexity of tree structures in three dimensions. Consequently, the application of function (3) is limited. Alternatively, function (3) can be redefined in terms of the vegetative surface area of a whole tree $[S(D, h)]$ and the relative distribution of vegetative surface area $[\psi_S(x_1, x_2, x_3)]$ given by:

$$S_{AD}(D,h,x_1,x_2,x_3) = \frac{S(D,h)}{\Delta x_1 \Delta x_2 \Delta x_3} \int_{x_3-0.5\Delta x_3}^{x_3+0.5\Delta x_3} \int_{x_2-0.5\Delta x_2}^{x_2+0.5\Delta x_2} \int_{x_1-0.5\Delta x_1}^{x_1+0.5\Delta x_1} \psi_S(x'_1,x'_2,x'_3)dx'_1dx'_2dx'_3 \quad (4)$$

The surface areas of trunk, branches, leaves, and seeds for any tree are measurable in the field; thus the vegetative surface area of a whole tree for a given species at a particular site can be estimated and statistically related to its DBH and height. However, the relative distribution of vegetative surface area remains difficult to estimate because it is not easy to measure the vegetative surface area in three dimensions under field conditions. It is desirable that the integral term in function (4) be defined as a combination of some 1- or 2-dimensional terms capable of being estimated in the field.

The lower the resolution of the grid cells, the easier it is to define the integral term in function (4). As the size of the grid cells increases, the resolution tends to be lower. As a result, it becomes easier to define the integral term. If the resolution is so low that one grid cell contains a while tree, or the dimensions of the cell (Δx_1, Δx_2, and Δx_3) are given by the maximum crown diameters in the width and length dimensions, and tree height, the integral term can be defined as '1'. Unfortunately, this resolution makes the structural description meaningless in addressing the arrangements of vegetative surface area and volume within a shelterbelt canopy. For meaningful structural description, higher resolution must be used. As the size of the grid cells decreases, the resolution tends to be higher and it becomes more difficult to define the integral term. The resolution should be increased to the degree necessary to provide a meaningful structural description while remaining feasible to define the integral term.

The grid cell sizes used in previous numerical simulations of boundary-layer flows near a shelterbelt are a reasonable reference point to determine the necessary resolution of the structural description for a tree shelterbelt. Assuming that the vegetative surface areas of hypothetical shelterbelts were distributed uniformly along the length dimension, Wang et al. (2001) subdivided the shelterbelt and the surrounding space into increments of 0.1 to 0.5 H across the width dimension (x_1) and of 0.1 H with the height dimension (x_3) for their simulations. If the variability in shelterbelt structure along the length dimension (x_2) is to be considered, the length dimension must also be divided. The distance between adjacent trees within a row can be the increment along the length dimension because it is small relative to length. Accordingly, the size of the grid cells is suggested as: $\Delta x_1 \leq 0.5\ H$ across the width dimension, $\Delta x_2 = d_t$ (where d_t is the distance between adjacent trees within a row) along the length dimension, and $\Delta x_3 \leq 0.1\ H$ with the height dimension.

By subdividing a shelterbelt into numerous grid cells at the suggested size, we can now use two distributions, which are capable of being measured and estimated, to define the integral term in function (4): (1) the marginal relative distribution of vegetative surface area with height $[\psi_{S3}(x_3)]$ and (2) the marginal relative distribution of vegetative surface area across the width dimension at a given height $[\psi_{S13}(x_1|x_3)]$. Then:

$$\psi_{S3}(x_3) = \int_{-\infty}^{+\infty} \int_{-\infty}^{+\infty} \psi_S(x'_1,x'_2,x'_3)dx'_1dx'_2 \quad (5)$$

and

$$\psi_{S13}(x_1|x_3) = \frac{\int_{-\infty}^{+\infty} \psi_S(x'_1,x'_2,x'_3)dx'_2}{\psi_{S3}(x_3)} \quad (6)$$

The distribution, $\psi_{S3}(x_3)$, describes the relative allocation of vegetative surface area of a whole tree with height. Its integration from the ground to the top of a tree equals one. Integration from bottom to top of a grid cell gives the relative vegetative surface area within the layer with respect to the entire tree (term [2] in function (7)). It can be found by measuring the tree surface area layer by layer with height. The distribution, $\psi_{S13}(x_1|x_3)$, describes the relative allocation of vegetative surface area across the width dimension at a given height of x_3. Its integration from one side to the other of a tree across the width dimension at any height equals one. The integration of its average over height of a grid cell from one side to the other, both of which are parallel to the length dimension, is the relative vegetative surface area in the grid cell with respect to the layer (term [3] in function (7)). This distribution can also be found if the vegetative surface area in a layer is measured section by section across the width dimension. Therefore, function (4) can be defined using three 1- or 2-dimensional terms capable of being measured and estimated under field conditions:

$$S_{AD}(D,h,x_1,x_2,x_3) = \frac{1}{\Delta x_1 \Delta x_2 \Delta x_3} \underset{[1]}{[S(D,h)]} \underset{[2]}{\left[\int_{x_3-0.5\Delta x_3}^{x_3+0.5\Delta x_3} \psi_{S3}(x'_3)dx'_3\right]} \underset{[3]}{\left[\int_{x_1-0.5\Delta x_1}^{x_1+0.5\Delta x_1} \frac{1}{\Delta x_3}\int_{x_3+0.5\Delta x_3}^{x_3+0.5\Delta x_3} \psi_{S13}(x'_1|x'_3)dx'_3dx'_1\right]} \tag{7}$$

Given DBH and height, this function spatially describes the vegetative surface area density for an individual tree composed of trunk, branches, leaves, and seeds. Its right hand side can be separated into four parts for these four tree components:

$$\begin{aligned} S_{AD}(D,h,x_1,x_2,x_3) = \frac{1}{\Delta x_1 \Delta x_2 \Delta x_3} \Bigg\{ & \underset{[1]}{[S_T(D,h)]} \underset{[2]}{\left[\int_{x_3-0.5\Delta x_3}^{x_3+0.5\Delta x_3} \psi_{ST3}(x'_3)dx'_3\right]} \underset{[3]}{\left[\int_{x_1-0.5\Delta x_1}^{x_1+0.5\Delta x_1} \frac{1}{\Delta x_3}\int_{x_3+0.5\Delta x_3}^{x_3+0.5\Delta x_3} \psi_{ST13}(x'_1|x'_3)dx'_3dx'_1\right]} \\ & + \underset{[4]}{S_B(D,h)} \underset{[5]}{\left[\int_{x_3-0.5\Delta x_3}^{x_3+0.5\Delta x_3} \psi_{SB3}(x'_3)dx'_3\right]} \underset{[6]}{\left[\int_{x_1-0.5\Delta x_1}^{x_1+0.5\Delta x_1} \frac{1}{\Delta x_3}\int_{x_3+0.5\Delta x_3}^{x_3+0.5\Delta x_3} \psi_{SB13}(x'_1|x'_3)dx'_3dx'_1\right]} \\ & + \underset{[7]}{S_L(D,h)} \underset{[8]}{\left[\int_{x_3-0.5\Delta x_3}^{x_3+0.5\Delta x_3} \psi_{SL3}(x'_3)dx'_3\right]} \underset{[9]}{\left[\int_{x_1-0.5\Delta x_1}^{x_1+0.5\Delta x_1} \frac{1}{\Delta x_3}\int_{x_3+0.5\Delta x_3}^{x_3+0.5\Delta x_3} \psi_{SL13}(x'_1|x'_3)dx'_3dx'_1\right]} \\ & + \underset{[10]}{S_S(D,h)} \underset{[11]}{\left[\int_{x_3-0.5\Delta x_3}^{x_3+0.5\Delta x_3} \psi_{SS3}(x'_3)dx'_3\right]} \underset{[12]}{\left[\int_{x_1-0.5\Delta x_1}^{x_1+0.5\Delta x_1} \frac{1}{\Delta x_3}\int_{x_3+0.5\Delta x_3}^{x_3+0.5\Delta x_3} \psi_{SS13}(x'_1|x'_3)dx'_3dx'_1\right]} \Bigg\} \end{aligned} \tag{8}$$

where $S_T(D, h)$, $S_B(D, h)$, $S_L(D, h)$, and $S_S(D, h)$ are the vegetative surface areas of trunk, branches, leaves, and seeds of a whole tree, respectively. The functions $\psi_{ST3}(x_3)$, $\psi_{SB3}(x_3)$, $\psi_{SL3}(x_3)$, and $\psi_{SS3}(x_3)$ are the marginal relative distributions of vegetative surface areas with height for trunk, branches, leaves, and seeds, respectively. Their integrations denoted by terms [2], [5], [8], and [11] are the relative vegetative

surface areas in a given layer with respect to an entire tree for the corresponding components. The functions $\psi_{ST13}(x_1|x_3)$, $\psi_{SB13}(x_1|x_3)$, $\psi_{SL13}(x_1|x_3)$, and $\psi_{SS13}(x_1|x_3)$ are the marginal relative distributions of vegetative surface areas across the width dimension at a given height for trunk, branches, leaves, and seeds, respectively. Their integrations denoted by terms [3], [6], [9], and [12] are the relative vegetative surface areas in a given grid cell with respect to the layer for the corresponding terms.

Using the same derivation procedure, the cubic density $[\beta_c(D, h, x_1, x_2, x_3)]$, in a grid cell centered at (x_1, x_2, x_3) with dimensions Δx_1, Δx_2, and Δx_3 (Figure 6) for a given tree species with known DBH and height at a particular site can be defined as:

$$\begin{aligned}\beta_C(D,h,x_1,x_2,x_3) = \frac{1}{\Delta x_1 \Delta x_2 \Delta x_3} \Bigg\{ & V_T(d,h)\left[\int_{x_3-0.5\Delta x_3}^{x_3+0.5\Delta x_3} \psi_{VT3}(x_3')dx_3'\right]\left[\int_{x_1-0.5\Delta x_1}^{x_1+0.5\Delta x_1} \frac{1}{\Delta x_3}\int_{x_3+0.5\Delta x_3}^{x_3+0.5\Delta x_3} \psi_{VT13}(x_1' \mid x_3')dx_3'dx_1'\right] \\ & + V_B(d,h)\left[\int_{x_3-0.5\Delta x_3}^{x_3+0.5\Delta x_3} \psi_{VB3}(x_3')dx_3'\right]\left[\int_{x_1-0.5\Delta x_1}^{x_1+0.5\Delta x_1} \frac{1}{\Delta x_3}\int_{x_3+0.5\Delta x_3}^{x_3+0.5\Delta x_3} \psi_{VB13}(x_1' \mid x_3')dx_3'dx_1'\right] \\ & + V_L(d,h)\left[\int_{x_3-0.5\Delta x_3}^{x_3+0.5\Delta x_3} \psi_{VL3}(x_3')dx_3'\right]\left[\int_{x_1-0.5\Delta x_1}^{x_1+0.5\Delta x_1} \frac{1}{\Delta x_3}\int_{x_3+0.5\Delta x_3}^{x_3+0.5\Delta x_3} \psi_{VL13}(x_1' \mid x_3')dx_3'dx_1'\right] \\ & + V_S(d,h)\left[\int_{x_3-0.5\Delta x_3}^{x_3+0.5\Delta x_3} \psi_{VS3}(x_3')dx_3'\right]\left[\int_{x_1-0.5\Delta x_1}^{x_1+0.5\Delta x_1} \frac{1}{\Delta x_3}\int_{x_3+0.5\Delta x_3}^{x_3+0.5\Delta x_3} \psi_{VS13}(x_1' \mid x_3')dx_3'dx_1'\right]\Bigg\}\end{aligned} \tag{9}$$

The terms in this function are defined analogous to those in function (8) with '*V*' indicating volume.

Functions (8) and (9) are working models to define the spatial functions of vegetative surface area density and cubic density of a common tree in a shelterbelt. Both working models provide guidance on how to estimate the structural descriptors of a tree shelterbelt for the prediction of the wind fields in its sheltered areas. To estimate the structural descriptors for a given tree shelterbelt at the resolution as determined by the suggested grid cell size, we need to develop the 24 sub-functions in both models for calculating the corresponding 24 terms for each tree in the shelterbelt. The 24 sub-functions are dependent on tree species, age, site condition, planting pattern, and management. For a given shelterbelt at a particular site, the 24 sub-functions need to be explicitly expressed in terms of DBH, tree height, and/or spatial variables for each tree species. The development of the 24 sub–functions for a given shelterbelt goes beyond the scope of this paper and were reported separately (Zhou et al. 2002).

Summary and conclusion

If we are to address the aerodynamic influence of a tree shelterbelt, we must have the capability of predicting the wind flow associated with the shelterbelt structure. The structural description of a tree shelterbelt is critical to this capability. This description has been expressed in two dimensions using optical porosity (or optical density); however, it is insufficient to represent the aerodynamic influence of tree shelterbelts with complex 3D structures. An analysis of numerous studies indicates that: (1) shelterbelts with different lengths, heights, widths, or cross-sectional shapes but similar internal structural components produce different wind fields; (2) vegetative surfaces extract momentum from and exert shear stress on wind flow through a shelterbelt canopy, and the arrangement of these surfaces determines the spatial distribution of the extraction and exertion; (3) vegetative volume and its arrangement are responsible for the divergence and convergence of air flow around and through a shelterbelt canopy; and (4) the geometric shape of the elements in a shelterbelt sig-

nificantly influences the wind field close to the barrier. Therefore, we propose that *the aerodynamic structure of a tree shelterbelt in three dimensions should be defined by the external structural characteristics: length, height, width, and cross-sectional shape; and by the internal structural components: amounts and arrangements of its vegetative surface area and volume as well as the geometric shape of individual vegetative elements.*

In order to associate the overall structure of a tree shelterbelt with wind speed, turbulent stress, and pressure, the defined structure needs to be quantitatively characterized. The spatial functions of vegetative surface area density and cubic density are proposed as the two structural descriptors best able to characterize the overall 3D aerodynamic structure of a tree shelterbelt because they can not only describe the internal structural components of the shelterbelt, but also indicate the external structural characteristics of the shelterbelt. Two working models for guiding the field estimation are developed, defining both structural descriptors of a common tree in a shelterbelt in three dimensions using the three types of 1- or 2-dimensional sub-functions. For vegetative surface area or volume, the three types of sub-functions describe the amount, marginal relative distribution with height, and marginal relative distribution across the width dimension at a given height. Based on field measurements, these sub-functions can be defined.

Describing the 3D aerodynamic structure of a tree shelterbelt using the developed models based on field measurements is labor intensive. An efficient indirect method to estimate this structure is needed. The definition and characterization of the 3D aerodynamic structure provide a theoretical basis from which the indirect method can be developed. The working models provide guidance for estimating the actual structure of a tree shelterbelt against which the indirect method can be verified. Moreover, the actual structure can be used to further test the shelterbelt turbulent flow model previously tested using assumed vegetative surface area density (Takle et al. 2003), advancing our understanding of the boundary-layer flows as influenced by a shelterbelt.

Acknowledgements

A contribution of the University of Nebraska Agricultural Research Division, Lincoln, Nebraska, USA. Journal Series No. 13336. This research was supported in part by funds provided through USDA/CSRS NRI Competitive Grants (#93-37101-8954 and #96-35209-3892) and the McIntyre-Stennis Forestry Research Program. The authors gratefully acknowledge the review by Drs. B.L. Blad, M.M. Schoeneberger, E. Blankenship, and four anonymous reviewers.

References

Bean A., Alperi R.W. and Federer C.A. 1975. A method for categorizing shelterbelt porosity. Agric Meteorol 14: 417–429.

Brandle J.R., Hodges L. and Wight B. 2000. Windbreak practices. In: Garrett H.E., Rietveld W.J. and Fisher R.F. (eds), North American Agroforestry: An Integrated Science and Practice. American Society of Agronomy Inc., Madison, Wisconsin, USA, pp. 79-118.

Carbon J.M. 1960. The dependence of the shelter effect of shelterbelts on their structure. Fifth World Forestry Congress Proceedings 3: 1662–1664.

Cao S.S., Lei Q.D. and Jiang F.Q. 1981a. Field determinations of the optimum porosity and cross-sectional shape of a shelterbelt. Bulletin of the Institute of Forestry and Pedology, Academia Sinica, Science Press, Beijing 5: 9–19. (In Chinese with French abstract).

Cao S.S., Yie S.S. and Zhu J.W. 1981b. Establishment and effectiveness of *Pinus tabulaeformis* shelterbelts. Bulletin of the Institute of Forestry and Pedology, Academia Sinica, Science Press, Beijing 5: 1-8. (In Chinese with French abstract).

Fu M.H., Jiang F.Q. and Yang R.Y. 1992. Study on porosity of poplar shelterbelts and its application in belts tending felling. In: Jiang F.Q. (ed.), Theory and Technology for Shelterbelt Management, Forestry Press of China, Beijing, pp. 102-108. (in Chinese with English abstract).

Gandemer J. 1979. Wind shelters. J Ind Aerodyn 4: 371–389.

George E.J., Broberg D. and Worthington E.L. 1963. Influence of various types of field windbreaks on reducing wind velocities and depositing snow. J For 61: 345–349.

Gloyne R.W. 1955. Some effects of shelter-belts and wind-breaks. Meteorol Mag 84: 272–281.

Gross G. 1987. A numerical study of the air flow within and around a single tree. Boundary-Layer Meteorol 40: 311–327.

Heisler G.M. and DeWalle D.R. 1988. Effects of windbreak structure on wind flow. Agric Ecosystems Environ 22/23: 41–69.

Jensen M. 1954. Shelter Effect: Investigations into the Aerodynamics of Shelter and its Effects on Climate and Crops. The Danish Technical Press, Copenhagen, Denmark, 264 pp.

Judd M.J., Raupach M.R. and Finnigan J.J. 1996. A wind tunnel study of turbulent flow around single and multiple windbreaks, part I: Velocity fields. Boundary-Layer Meteorol 80: 127–165.

Kozeny J. 1927. Über kapillare Leitung des Wassers im Boden (Aufstieg, Versicherung, und Anwendung auf die Bewässerung). Sber Akad Wiss Wien (Abt. IIa) 136: 271–306.

Lee X. 2000. Air motion within and above forest vegetation in non-ideal conditions. For Ecol Manage 135: 3–18.

Loeffler A.E., Gordon A.M. and Gillespie T.J. 1992. Optical porosity and windspeed reduction by coniferous windbreaks in Southern Ontario. Agrofor Syst 17: 119–133.

Miller D.R., Rosenberg N.J. and Bagley W.T. 1975. Wind reduction by a highly permeable tree shelterbelt. Agric Meteorol 14: 321–333.

Perera M.D.A.E.S. 1981. Shelter behind two-dimensional solid and porous fences. J Wind Eng Ind Aerodyn 8: 93–104.

Plate E.J. 1971. The aerodynamics of shelter belts. Agric Meteorol 8: 203–222.

Scheidegger A.E. 1974. The Physics of Flow through Porous Media, 3rd ed. University of Toronto Press, Toronto, Canada, 353 pp.

Schmidt R.A., Jairell R.L., Brandle J.R., Takle E.S. and Litvina I.V. 1995. Windbreak shelter as a function of wind direction. The Ninth Symposium on Meteorological Observations & Instrumentation, the American Meteorological Society, Boston, Massechussets, USA, pp. 269–274.

Schwartz R.C., Fryrear D.W., Harris B.L., Bilbro J.D. and Juo A.S.R. 1995. Mean flow and shear stress distributions as influenced by vegetative windbreak structure. Agric For Meteorol 75: 1–22.

Stoeckeler J.H. 1962. Shelterbelt Influence on Great Plains Field Environment and Crops. USDA Forest Service, Production Research Report No. 62, 26 pp.

Sturrock J.W. 1969. Aerodynamic studies of shelterbelts in New Zealand-1: low to medium height shelterbelts in Mid-Canterbury. New Zealand J Sci 12: 754–776.

Sturrock J.W. 1972. Aerodynamic studies of shelterbelts in New Zealand-2: Medium-height to tall shelterbelts in Mid Canterbury. New Zealand J Sci 15: 113–140.

Tabler R.D. and Veal D.L. 1971. Effect of snow fence height on wind speed. Bulletin of the International Association of Scientific Hydrology 16: 49–56.

Takahashi H. 1978. Wind tunnel test on the effect of width of windbreaks on the wind speed distribution in leeward. J Agr Met 33: 183–187.

Takle E.S., Falk M.J., Zhou X.H. and Brandle J.R. 2003. Calibration and applications of a shelterbelt turbulent flow model. In Ruck B., Kottmeier C., Mattheck C., Quine C. and Wilhelm G. (eds), Proceedings of the International Conference on Wind Effects on Trees. Institute of Hydromechanics, University of Karlsruhe, Germany, pp. 57–64.

Wang H., Takle E.S. and Shen J.M. 2001. Shelterbelts and windbreaks: Mathematical modeling and computer simulations of turbulent flows. Annu Rev Fluid Mech 33: 549–586.

Wilson J.D. 1987. On the choice of a windbreak porosity profile. Boundary-Layer Meteorol 38: 37–49.

Wilson N.R. and Shaw R.H. 1977. A higher order closure model for canopy flow. J Applied Meteorol 16: 1197–1205.

Woodruff N.P. and Zingg A.W. 1952. Wind-Tunnel Studies of Fundamental Problems Related to Windbreaks. USDA Soil Conservation Service, SCS-TP-112, 25 pp.

Woodruff N.P. and Zingg A.W. 1953. Wind tunnel studies of shelterbelt models. J. For. 51: 173–178.

Woodruff N.P., Fryrear D.W. and Lyles L. 1963. Reducing Wind Velocity with Field Shelterbelts. USDA Agricultural Research Service, Technical Bulletin 131, 26 pp.

Xiang K.F. and Zhou X.H. 1990. The effect of protective forest for pasture: Aerodynamics, thermodynamics and hydrology. In: Xiang K.F., Shi J.C., Baer N.W. and Sturrock J.W. (eds), Protective Plantation Technology. Publishing House of Northeast Forestry University, Harbin, pp. 238-245.

Zhang H., Brandle J.R., Meyer G.E. and Hodges L. 1995. The relationship between open windspeed and windspeed reduction in shelter. Agrofor Syst. 32: 297–311.

Zhou X.H., Brandle J.R., Takle E.S. and Mize C.W. 2004. Relationship of three-dimensional structure to shelterbelt function: A theoretical hypothesis. J. Crop. Production. (In press).

Zhou X.H., Brandle J.R., Takle E.S. and Mize C.W. 2002. Estimation of the three-dimensional aerodynamic structure of a green ash shelterbelt. Agric For Meteorol 111: 93–108.

Zhu T.Y. 1981. Wind tunnel observations on the aerodynamic influences of a shelterbelt. Bulletin of the Institute of Forestry and Pedology, Academia Sinica, Science Press, Beijing 5: 29–46. (In Chinese with French abstract).